Published in final edited form as:
Dev Dyn. 2013 December ; 242(12): 1466–1477. doi:10.1002/dvdy.24059.

A Requirement for Commissureless2 Function during Dipteran Insect Nerve Cord Development

Joseph Sarro[1], **Emily Andrews**[2], **Longhua Sun**[1], **Susanta K. Behura**[1], **John C. Tan**[1], **Erliang Zeng**[3], **David W. Severson**[1,2], and **Molly Duman-Scheel**[1,2,4]

[1]Eck Institute for Global Health and Department of Biological Sciences, University of Notre Dame, Notre Dame, Indiana, 46556

[2]Department of Medical and Molecular Genetics, Indiana University School of Medicine, South Bend, Indiana, 46617

[3]Department of Computer Science and Engineering, University of Notre Dame, Notre Dame, IN, 46556

Abstract

Background—In Drosophila melanogaster, commissureless *(comm)* function is required for proper nerve cord development. Although *comm* orthologs have not been identified outside of *Drosophila* species, some insects possess orthologs of *Drosophila comm2*, which may also regulate embryonic nerve cord development. Here, this hypothesis is explored through characterization of *comm2* genes in two disease vector mosquitoes.

Results—*Culex quinquefasciatus* (West Nile and lymphatic filiariasis vector) has three *comm2* genes that are expressed in the developing nerve cord. *Aedes aegypti* (dengue and yellow fever vector) has a single *comm2* gene that is expressed in commissural neurons projecting axons toward the midline. Loss of *comm2* function in both *A. aegypti* and *D. melanogaster* was found to result in loss of commissure defects that phenocopy the *frazzled (fra)* loss of function phenotypes observed in both species. Loss of *fra* function in either insect was found to result in decreased *comm2* transcript levels during nerve cord development.

Conclusions—The results of this investigation suggest that Fra downregulates repulsion in precrossing commissural axons by regulating *comm2* levels in both *A. aegypti* and *D. melanogaster*, both of which require Comm2 function for proper nerve cord development,

Keywords

commissureless; development; nervous system; mosquito; *Aedes aegypti*; *Culex quinquefasciatus*; *Drosophila melanogaster*; *frazzled*

INTRODUCTION

In recent years, knockdown studies have suggested that axon guidance gene function has diverged in the insect embryonic ventral nerve cord (Clemons et al., 2011; Haugen et al., 2011; Evans and Bashaw, 2012). For example, an siRNA-mediated knockdown strategy was used to study the role of the Netrin receptor *frazzled (fra)* during *Aedes aegypti* embryonic nerve cord development (Clemons et al., 2011). The results of this investigation, the first targeted knockdown of a gene during vector mosquito embryogenesis, suggest that although

[4]To whom correspondence should be addressed: mscheel@nd.edu, Indiana University School of Medicine-South Bend at Notre Dame, Raclin-Carmichael Hall, 1234 Notre Dame Ave., South Bend, IN 46617, Phone: (574) 631-7194, Fax: (574) 631-7821.

Fra plays a critical role during development of the *A. aegypti* ventral nerve cord, mechanisms regulating embryonic commissural axon guidance have diverged in dipteran insects. Specifically, loss of *Aae fra* results in thin and missing commissural axons, defects which are qualitatively similar to those observed in *D. melanogaster fra* null mutants. However, complete commissure loss is observed in *A. aegypti fra* knockdown embryos, which bear more resemblance to the *Drosophila commissureless (comm)* loss of function phenotype (Seeger et al., 1993) than the *Drosophila fra* loss of function phenotype (Kolodziej et al., 1996).

Mutations in the *D. melanogaster comm* gene were initially uncovered from a screen for mutations that affect development of the *Drosophila* embryonic CNS axons pathways (Seeger et al., 1993). The *comm* gene is the most extensively studied of the three *comm* family genes (*comm, comm2,* and *comm3*) in *D. melanogaster* (Keleman et al., 2002). Mutants for *comm* display a unique phenotype, the complete absence of most axon commissures. Cloning and sequencing of the *comm* gene revealed that it encodes a novel transmembrane protein (Tear et al., 1996). Subsequent studies revealed that Comm functions in neurons to regulate the intracellular trafficking and surface levels of Robo (Keleman et al., 2002; McGovern and Seeger, 2003; Keleman et al., 2005), receptor for the midline repellent Slit. The choice of crossing (commissural) or noncrossing (ipsilateral) axon pathways is regulated by the differential sensitivity of axons to Slit (reviewed by (Dickson, 2002). Ipsilateral axons lacking Comm expression are repelled by Slit-Robo signaling and fail to cross the midline. Commissural axons, which express Comm and consequently lack Robo surface expression, are initially insensitive to Slit-mediated repulsion and respond to Net attractive midline cues. Once commissural axons reach the midline, Comm expression is downregulated, and these neurons are repelled from the midline by Slit-Robo signaling (Kidd et al., 1999; Stein and Tessier-Lavigne, 2001; Dickson and Gilestro, 2006). Thus, the ability of Comm to control Robo levels is critical for proper nerve cord formation.

Despite the importance of *comm* gene function in the *D. melanogaster* nerve cord, no *comm* gene ortholog has been detected outside of the *Drosophila* species (Waterhouse et al., 2013). However, orthologs of the *Drosophila comm2* and *comm3* genes, neither of which have been extensively characterized in *Drosophila*, have been identified in other arthropods, including vector mosquitoes (Behura et al., 2011). It was hypothesized that these *comm* family genes might function during vector mosquito nerve cord development. In this investigation, we perform phylogenetic and expression analyses of *comm* family orthologs in *C. quinquefasciatus* and *A. aegypti*. The role of the *A. aegypti comm2* gene, the only *comm* family ortholog in this species, was assessed through siRNA-mediated silencing. The function of *Aae comm2* was compared to that of its closest *D. melanogaster comm* family ortholog, *D. melanogaster comm2*, which was also assessed for comparison.

RESULTS AND DISCUSSION

Mosquito *comm* family genes

Previous comparative genomic analyses of developmental genes in the *D. melanogaster, A. aegypti, C. quinquefasciatus,* and *A. gambiae* genomes revealed changes in the number of axon guidance genes in these species (Behura et al., 2011). While three *comm* family genes *(comm, comm2,* and *comm3)* are found in *D. melanogaster*, no *comm* family genes have been identified in *A. gambiae.* However, three *comm* family genes were identified in *C. quinquefasciatus (CPIJ016283, CPIJ016285, CPIJ017280),* while a single *comm* family gene has been identified in the *A. aegypti* genome *(AAEL007250).* These genes were noted to be *Drosophila comm2/comm3* orthologs (Behura et al., 2011). Sequence analyses were performed to further explore the relationship between these mosquito *comm* family genes with each other and with those of other arthropods (Fig. 1).

The amino acid sequence conservation pattern among *Drosophila* and mosquito Comm family proteins is shown in Fig. 1A, C. Phylogenetic comparisons suggest that the *A. aegypti* and *C. quinquefasciatus* Comm family proteins more closely resemble each other than they do any of the *Drosophila* Comm family proteins (Fig. 1B, C). *D. melanogaster* Comm family proteins bear a highly conserved 22 amino acid sequence (residues 215–236 in *D. melanogaster* Comm; Keleman et al., 2002). This sequence is well conserved in AAEL007250, CPIJ16283, and CPIJ16285 (Fig. 1A). However, comparison of the motif maps of CPIJ017280 with *D. melanogaster* Comm2 (FBgn0041160) based on Dayhoff weight estimates of local sequence similarities (Leontovich *et al*. 1993) revealed that the conserved cytoplasmic domain is either lost or extensively mutated in CPIJ017280 protein (Fig. 1A and data not shown). The *D. melanogaster* Comm protein also contains a heterotetrameric adaptor protein binding site motif LPSY (Wolf et al., 1998) which is conserved in *D. melanogaster* Comm2, but not Comm3. This domain is required for endosomal sorting of Comm and Comm2, as well as downregulation of Robo and the promotion of midline crossing (Keleman et al., 2002; Choi et al., 2003). An LPSY motif is found in all of the *A. aeygpti and C. quinquefasciatus* Comm family proteins, suggesting that with reference to this functionally significant motif, these proteins are more comparable to *D. melanogaster* Comm2 than Comm3. This observation suggests that the *A. aegypti* and *C. quinquefasciatus* genes are *comm2* orthologs.

A *comm2* orthology assignment is supported by OrthoDB for all of the *A. aegypti* and *C. quinquefasciatus comm* family genes except *CPIJ16283,* which is referred to as a *comm3* ortholog (Waterhouse et al., 2013). Still, given the presence of the LPSY motif in CPIJ16283 and our phylogenetic analyses which group it most closely with AAEL007250 (Fig. 1B), we argue that *comm2* orthology assignments for all of the three *C. quinquefasciatus* genes is appropriate. Thus, in addition to naming *AAEL007250 Aae comm2*, we will refer to *CPIJ16283* as *Cqu comm2a, CPIJ16285* as *Cqu comm2b,* and *CPIJ017280* as *Cqu comm2c*. Moreover, in addition to the detection of brain and head tissue expression of all these genes, analysis of their expression in developing mosquito embryonic nerve cords suggests that they may function to regulate development of this tissue (Fig. 2, 3), a hypothesis which is functionally examined in *A. aegypti* in this investigation (see below). Functional testing of this hypothesis in *C. quinquefasciatus*, which could further support or potentially refute the *comm2* orthology assignment of these genes, will be interesting. However, this will first require optimization of knockdown methodology in *C. quinquefasciatus* embryos.

In summary, these sequence analysis studies revealed that despite the lack of a detectable *comm* family gene ortholog in *A. gambiae, C. quinquefasciatus* has three *comm2* genes, while *A. aegypti* has one. Interestingly, a single *comm* family gene, a probable *comm2* ortholog, has been discovered in *Anopheles darlingi* (Fig. 1B, C, Lawson et al., 2009), suggesting that *comm* genes were not lost in all anopheline mosquitoes. We of course cannot eliminate the possibility that an *A. gambiae comm* family gene exists, but has not yet been detected due to sequencing gaps. This possibility aside, one likely explanation for these combined findings is that a single *comm2* gene existed when the *Drosophila* and mosquito lineages split. Some mosquito species retained the single gene (i.e. *A. aegypti* and *A. darlingi),* and others lost it *(A. gambiae),* while the *comm* gene family expanded in *C. quinquefasciatus* and *D. melanogaster*. In addition, it is likely that the *comm2* gene family in *C. quinquefasciatus* may be evolving faster than the *comm* family of other dipterans. By estimating evolutionary distance in a pair-wise manner between species, it was found that the *C. quinquefasciatus* Comm2 family has a relatively higher number of amino acid substitutions per site than other insects (Table 1). The data presented in Table 1 demonstrate that the pair-wise distances among the three *C. quinquefasciatus* Comm2 proteins are consistently higher than the pair-wise distances of Comm2 proteins within *Drosophila* or

between *Drosophila* and *A. aegypti*. Hence, the *C. quinquefasciatus* proteins distinctly differ in the rate of amino acid substitutions compared to that of *A. aegypti* or *Drosophila*.

Detailed analysis of *comm2* expression during *A. aegypti* nerve cord development

Given the lack of a detectable *comm* gene outside the drosophilids and the apparent lack of any *comm* family *(comm, comm2,* or *comm3)* gene in some insects (Behura et al., 2011; Evans and Bashaw, 2012), it is possible that the requirement for *comm* family gene function is not retained outside of *Drosophila*. However, given the expansion of *C. quinquefasciatus comm2* genes, all of which are expressed in the developing nerve cord (Fig. 2), it is also possible that *comm* family gene function is in fact required outside of *D. melanogaster,* a concept which has never been experimentally tested. To explore this, we opted to assess *comm2* gene function in *A. aegypti* because it has retained a single *comm* family ortholog (Fig. 1), and also due to the fact that we recently optimized embryonic knockdown strategies in this species (Clemons et al., 2010a; Clemons et al., 2011; Haugen et al., 2011; Nguyen et al., 2013), which is to our knowledge the only mosquito species in which embryonic RNAi knockdown studies have been published to date.

First, *Aae comm2* expression was assessed in detail during *A. aegypti* embryonic CNS development. Like the *Cqu comm2a, b,* and *c* genes (Fig. 2), *Aae comm2* is expressed in the brain and overlying head tissue and in many neurons of the embryonic nerve cord at the onset of commissural axon guidance toward the midline (Fig. 3A). Expression levels of *Aae comm2* in the developing nerve cord peak at ~50 hours (Fig. 3B) and then begin to subside (Fig. 3C). Nerve cord expression of *Aae comm2* has diminished by ~54 hrs (Fig. 3D), which corresponds to the time at which most axons have reached the midline (Clemons et al., 2011). These aspects of the *Aae comm2* ventral nerve cord expression pattern are quite similar to that which has been described for *D. melanogaster comm,* which has been extensively characterized (Keleman et al., 2002), with the exception that *D. melanogaster comm* has very prominent midline expression, the levels of which are often stronger than *comm* expression in more lateral neurons (Keleman et al., 2002). The expression pattern suggests that *Aae comm2* functions primarily in neurons and not in midline cells, which is consistent with the finding that *D. melanogaster comm* function is required in neurons, but not at the midline (Keleman et al., 2002).

D. melanogaster comm expression has been assessed in detail in both crossing and non-crossing axons (Keleman et al., 2002). These expression studies indicated that *D. melanogaster comm* is not expressed in non-crossing axons, but is detected specifically in commissural neurons as they are being guided to the midline and later extinguished after midline crossing. To determine if *Aae comm2* is expressed in a comparable manner, we first needed to identify crossing and non-crossing neurons in the ventral nerve cord of this species. Analysis of Even-skipped (Eve) expression has facilitated identification of homologous neurons in a wide variety of arthropods (Duman-Scheel and Patel, 1999). The Eve expression pattern is well conserved in *A. aegypti* (Fig. 4), which allowed for the identification of specific neurons. The Eve-positive RP2, aCC, pCC, U, and EL neurons do not cross the midline and do not express *comm* in *D. melanogaster* (Keleman et al., 2002). These neurons, all of which are also marked by Eve expression in *A. aegypti*, do not express *Aae comm2* (Fig. 4A, B, D). Several *comm2*-positive homologous cells were identified based on their positional locations with respect to Eve-expressing neurons in the *A. aegypti* nerve cord. The EG (Fig. 4A), RP1, RP3, and RP4 neurons (Fig. 4C), all of which cross the midline, were found to express *Aae comm2*. These expression analyses suggest that *Aae comm2*, like *D. melanogaster comm*, is expressed in crossing but not non-crossing neurons. Moreover, *Aae comm2* expression fades by the time that axons have reached the midline

(Fig. 3D), which presumably facilitates Slit-Robo mediated axon repulsion from the midline as it does in *Drosophila* (Keleman et al., 2002).

Knockdown of *comm2* in *A. aegypti* results in a commissureless phenotype

Expression data (Fig. 3,4) support the notion that *Aae comm2* function is required during nerve cord development. To examine this possibility, the putative role of *Aaecomm2* was assessed through siRNA-mediated knockdown experiments, which were recently shown to be an effective method of inhibiting gene expression during embryonic development of *A. aegypti* (Clemons et al., 2011; Haugen et al., 2011; Nguyen et al., 2013). Experimental or control siRNAs were microinjected at the pre-cellular blastoderm stage. Two siRNAs corresponding to different regions of the *Aae comm2* gene, *comm2*-siRNA 1 and *comm2*-siRNA 2, were used to target this gene. Control experiments were performed using previously designed control siRNA (Nguyen et al., 2013) which does not bear high sequence similarity to other genes in the *A. aegypti* genome. 53 hour old embryos were assessed post-injection of *comm2*-siRNA 1, comm2-siRNA 2, or control siRNA. *In situ* hybridization assays demonstrated that a majority of *comm2*-siRNA 1 (79%, n=33) and *comm2*-siRNA 2 (74%, n=31) injected embryos lacked *comm2* expression in the developing ventral nerve cord (Fig. 5B, C), while control-injected embryos displayed *comm2* expression levels which resemble those of wild-type embryos (Fig. 5A, n=46).

The impact of *comm2* knockdown on *A. aegypti* embryonic nerve cord development was assessed through anti-acetylated tubulin staining at 53 hours of development. Although control-injected animals had normal nerve cord development (n=71, Fig. 5D, F, Table 2), commissure formation was disrupted in embryos injected with either *comm2*-siRNA 1 (n=35, Fig. 5E, G) or siRNA 2 (n=51, Fig. 5H). Comparable phenotypes were generated through injection of *comm2*- siRNA 1 or 2 (Fig. 5E, G, H), suggesting that the commissureless phenotype observed was not the result of off-site targeting by either siRNA. 71% of *comm2*-siRNA 1 injected embryos and 51% of *comm2*-siRNA 2 injected embryos displayed severe nerve cord phenotypes in which most segments had commissure defects. Individual segments were scored in a subset of these animals, and the percentages of segments with moderate (thinning of commissures) or severe (loss/near loss) phenotypes are provided in Table 2. These data indicate that *Aae* Comm2 function is required for proper commissure formation in *A. aegypti.*

D. melanogaster comm2 is also required for nerve cord development

The results of the *A. aegypti* knockdown experiments suggested that *D. melanogaster* Comm2, the ortholog of *Aae* Comm2, may also function during nerve cord development. Expression of *D. melanogaster comm2* transcript is detected in the developing embryonic nerve cord (Fig. 6A, B), brain, and head tissue (not shown) in a pattern which resembles that of *Aae comm2* (Fig. 3). High levels of *D. melanogaster comm2* transcript are detected in the nerve cord at stage 13 (Fig. 6A), and by Stage 15, expression of *comm2* is observed in a more restricted set of *D. melanogaster* neurons (Fig. 6B). Like *Aae comm2*, expression of *D. melanogaster comm2* diminishes once the majority of commissural axons have crossed the midline (Fig. 6B). It has been suggested both in the discussion of Keleman et al. (2002) and also in the doctoral thesis of Choi (2003) that *D. melanogaster* Comm2, like *D. melanogaster* Comm, prevents Robo from reaching the cell surface. If this is true, then *D. melanogaster* Comm2, like Comm (Keleman et al., 2002) should not be expressed in neurons which do not project axons toward the midline. This was assessed in *D. melanogaster* in the same manner in which it was examined in *A. aegypti* (Fig. 4), through the combined analysis of Eve and Comm2 expression during nerve cord development. The results of these experiments (Fig. 7) were comparable to those obtained for *A. aegypti* (Fig.

4). The *D. melanogaster* Eve-positive EL, U, aCC, pCC, and RP2 neurons lack expression of Comm2 (Fig. 7).

In his doctoral thesis, Choi (2003) suggested that loss of function mutations in *D. melanogaster comm2* result in commissure loss resembling that of the *comm* mutant (Seeger et al., 1993). Moreover, the *comm2* mutants that he described also displayed a general distortion of the nerve cord that is not observed in *comm* mutants. To confirm these observations, commissure formation was examined through analysis of two additional *comm2* mutant strains, *comm2[MB01146]* and *comm2[MI02284]* (see methods section for additional details), neither of which were described by Choi (2003). *comm2[MB01146]* mutant embryos display both significant commissure loss (Fig. 8B, Table 3) as well as a general distortion of the nerve cord. Animals that are heterozygous for the *comm2[MB01146]* mutation in combination with *Df(3L)BSC845* (Fig. 8C, D, Table 3), a deletion in the region, displayed a comparable loss of commissure phenotype. The percentage of segments with severe commissure loss observed in embryos of these two genotypes was not significantly different ($P>0.1$, Table 3). These results suggest that *comm2[MB01146]* is an amorphic allele. Significant commissure loss and distortion of the nerve cord was also observed in animals homozygous for *comm2[MI02284]* (Fig. 8E, Table 3). Animals heterozygous for *comm2[MI02284]* in combination with *Df(3L)BSC845* (Fig. 8F) have phenotypes that are comparable to those of *comm2[MI02284]* homozygotes (Fig. 8E). The percentage of segments with severe commissure loss observed in embryos of these two genotypes was not significantly different ($P>0.1$, Table 3), suggesting that the *comm2[MI02284]* allele is also an amorphic *comm2* allele. These results, in combination with those of Choi (2003), demonstrate that Comm2 is required for nerve cord formation in *D. melanogaster*.

These analyses suggest that the function of Comm2 is generally well conserved between *A. aegypti* and *D. melanogaster*. However, it is noted that the nerve cord has an overall more distorted appearance in *D. melanogaster comm2* mutants (Fig. 8), which also display frequent breaks in the longitudinal connectives that were not observed in *A. aegypti comm2* knockdown embryos (Fig. 5E, G, H). Furthermore, the *D. melanogaster comm2* mutants assessed in this study had embryonic segments in which the few existing commissural axons passed into adjacent segments (one example in a *comm2[MB01146]/Df(3L)BSC845* heterozygote is shown in Fig. 8D). Thus, despite the generally well conserved function of Comm2 in the two species, some differences in the loss of function phenotypes do exist. Similar observations were made in our previous *fra* (Clemons et al., 2011) and *semaphorin-1a* (Haugen et al., 2011) investigations.

Loss of *frazzled* function results in loss of *comm2* expression in *D. melanogaster* and *A. aegypti*

In previous studies, we noted that the *A. aegypti fra* knockdown phenotype, in which both the anterior and posterior commissures were disrupted, resembles that of the *D. melanogaster comm* loss of function phenotype (Clemons et al., 2011). Here, we demonstrated that knockdown of *Aae comm2* results in commissure loss (Fig. 5E, G, H, Table 2) which resembles the *Aae fra* loss of function phenotype (Clemons et al., 2011). Likewise, loss of *D. melanogaster comm2* results in defective commissural axon guidance (Fig. 8B), and the *D. melanogaster comm2* (Fig. 8B) and *fra* loss of function mutant nerve cord phenotypes (Kolodziej et al., 1996) are notably similar. We have performed microarray experiments in which global changes in gene expression resulting from gain and loss of Fra signaling were assessed in *D. melanogaster* (see Experimental Procedures for approach/accession information; the comprehensive results of these studies will be presented in their entirety elsewhere). These experiments demonstrated that loss of *fra* resulted in a −0.10 log2

fold decrease in *comm2* expression, while activation of Net-Fra signaling resulted in a 0.20 log2 fold increase in *comm2* transcript levels. Although these fold changes were not statistically significant, these observations, when combined with the notable similarity of the *fra* and *comm2* mutant phenotypes in both *D. melanogaster* and *A. aegypti*, suggested that *comm2* expression levels may change in response to Fra signaling. Such a phenomenon has been described in relation to the *Drosophila comm* gene, the expression of which decreases in *Drosophila fra* mutants (Yang et al., 2009). Thus, *comm2* transcript levels were assessed in *fra[3]* loss of function *D. melanogaster* embryos through whole-mount *in situ* hybridization. These experiments demonstrated that loss of *fra* function results in substantial loss of *comm2* expression in the developing nerve cord (Fig. 9B, n=36). These results suggest that Fra downregulates repulsion in commissural axons that are being guided to the midline by regulating not only *comm*, but also *comm2* levels. Thus, in addition to mediating the response of Netrin attractive cues secreted from the midline, Fra signaling also downregulates responses to repulsive Slit-Robo cues by promoting high levels of both Comm and Comm2.

Assessment of *comm2* expression in *A. aegypti fra* knockdown embryos (Fig. 9D) demonstrated that the ability of Fra signaling to regulate *comm2* transcript levels is conserved between *D. melanogaster* and *A. aegypti*. Loss of *comm2* nerve cord expression was observed in 85% of *fra* knockdown siRNA-injected mosquito embryos (n=105). Thus, regulation of *comm* family gene transcript levels by Fra is observed outside of *Drosophila*. These findings demonstrate that although some insects lack an apparent *comm* family ortholog, the function of Comm2 is generally well conserved between *D. melanogaster* and *A. aegypti*, as evidenced through the well conserved expression patterns of *comm2* in *A. aegypti* (Figs. 3 and 4) and *D. melanogaster* (Figs. 6 and 7), the commissure loss phenotypes observed in the *comm2* loss of function nerve cords of both species (Figs. 5,8, Tables 2,3), and the finding that *comm2* levels are regulated by Fra signaling in both insects (Fig. 9).

Given that Comm2 plays an essential role in the developing *D. melanogaster* and *A. aegypti* nerve cord, it is interesting that *A. gambiae* and *T. castaneum* appear to lack a *comm* family gene (Behura et al., 2011; Evans and Bashaw, 2012). It is possible that genome sequencing gaps or the notably low level of amino acid conservation among Comm family proteins has hindered the identification of a *comm* family ortholog in these insects, and that they do possess a *comm* family gene that cannot be identified through sequence comparisons. Interestingly, although no *comm* family genes have yet been identified in vertebrates, RabGDI was recently found to regulate Robo1 surface expression levels in chick commissural axons (Philipp et al., 2012). These findings suggest that other proteins, perhaps even Rab GDI which has been described in insects (Ricard et al., 2001), may function to regulate Robo surface levels in animals which lack apparent Comm family proteins.

EXPERIMENTAL PROCEDURES

Sequence analyses

Mosquito *comm* orthologs were previously identified (Behura et al., 2011) from Biomart (Smedley et al., 2009) and Vectorbase (Lawson et al., 2009). The amino acid sequences of Comm family proteins were obtained from Vectorbase (Lawson et al., 2009) and Flybase (Tweedie et al., 2009). ClustalW (Chenna et al., 2003) was used for multiple sequence alignment. The phylogenetic tree was drawn using the Neighbor-Joining method (Saitou and Nei, 1987), and a bootstrap consensus tree was inferred from 1000 replicates (Felsenstein, 1992). The Poisson correction method (Zuckerkandl and Pauling, 1965) was used to compute evolutionary distances which correspond to the number of amino acid substitutions per site. Phylogenetic analyses were conducted using MEGA4 (Tamura et al., 2007). The pairwise distance between genes was also calculated using MEGA4. The local sequence

alignments for constructing motif maps of CPIJ016285 and CPIJ017280 in comparison with *D. melanogaster* Comm2 (FBgn0041160) was based on Dayhoff weight matrices (Leontovich *et al*. 1993) implemented in the GeneBee program (Brodsky *et al*. 1995).

Mosquito Rearing, Egg Collection, and Fixation

A. aegypti Liverpool- IB12 (LVP-IB12) and *C. quinquefasciatus* Johannesburg (JHB) strains, which were utilized in the genome sequencing efforts (Nene et al., 2007; Arensburger et al., 2010), were used in these studies. Mosquitoes were reared as previously described (Clemons et al., 2010b), except that an artificial membrane blood feeding system was employed. Procedures for *A. aegypti* embryo fixation (Clemons et al., 2010c) have been described, and these methods were applied to both *A. aegypti* and *C. quinquefasciatus* in this investigation. *C. quinquefasciatus* embryos were staged as previously described (Davis, 1967).

Drosophila Genetics

The following *D. melanogaster* mutant stocks were used in this investigation: *comm2[MB01146]* (Bloomington Stock Center, #23000), *comm2[MI02284]* (Bloomington Stock Center, #33190), *Df(3L)BSC845* (Bloomington Stock Center, #27888), and *fra[3]* (Bloomington Stock Center #8813). Detailed information about these stocks is available at Flybase (Tweedie et al., 2009). In summary, *comm2[MB01146]* and *comm2[MI02284]* are transgenic insertion stocks in the *comm2* locus produced by the *Drosophila* Gene Disruption Project that were derived by transposable element mobilization with the Dhyd\Minos-based constructs *Mi{ET1}* and *Mi{MIC}*, respectively (Metaxakis et al., 2005; Bellen et al., 2011). Levels of *comm2* transcript were not observed to be reduced in either strain, as is typical for Minos-generated alleles (Metaxakis et al., 2005). However, genetic characterization of these mutations described herein indicates that they behave as amorphic *comm2* alleles. *Df(3L)BSC845* is a large deletion of cytogenic region 71E1 which covers sequences 3L: 15,559,113 to 15,569,413 and results in the deletion of numerous genes, including *comm2* (Cook et al., 2012).

In situ hybridization, Immunohistochemistry, and Imaging

Riboprobes (~500 bp in size) corresponding to the following genes were synthesized as described (Patel, 1996): *Aae comm2 (AAEL007250), Cqu comm2* genes *CPIJ016283, CPIJ016285*, and *CPIJ017280*, and *D. melanogaster comm2 (CG7554). A. aegypti in situ* hybridization experiments were performed as discussed previously (Haugen et al., 2010), and this method was applied to *C. quinquefasciatus. D. melanogaster in situ* hybridization experiments were performed as described previously (Patel, 1996; VanZomeren-Dohm et al., 2008).

Immunohistochemistry was performed in *A. aegypti* using previously published methodology (Clemons et al., 2010d), and this protocol was applied to *C. quinquefasciatus. Drosophila* embryos were prepared and stained as described by Patel (Patel, 1994), who discusses the use of BP102 and anti-Even-skipped (Eve) 2B8 antibodies which he graciously provided. Anti-acetylated tubulin antibody was obtained from Zymed (San Francisco, CA). Anti-GFP antibody was purchased from Sigma-Aldrich (St. Louis, MO). The HRP-conjugated secondary antibodies used in this investigation were purchased from Jackson Immunoresearch (West Grove, PA). Use of GFP marked balancers permitted genotype scoring of *Drosophila* embryos in immunohistochemical assays.

Samples were imaged using a Zeiss Axioimager equipped with a Spot Flex camera or with a Zeiss LSM 710 Confocal Microscope. Images were processed with Adobe Photoshop and Zeiss ZEN Software.

RNAi knockdown experiments

Knockdown of *Aae comm2* was performed through embryonic microinjection of siRNAs corresponding to this gene as previously described in a protocol (Clemons et al., 2010a) which has been successfully utilized in three recent embryonic knockdown investigations (Clemons et al., 2011; Haugen et al., 2011; Nguyen et al., 2013). The following siRNAs corresponding to *Ae. aeygpti comm2* were synthesized by Dharmacon RNAi Technologies (Lafayette, CO): siRNA-1 sense: CGCCAGUGAUUUCAACCUGUU and antisense: CAGGUUGAAAUCACUGGCGUU (corresponds to base pairs 265–283 of *Aae comm2*) and siRNA-2 sense: CGACCUUCGGUCAUCAAACUU and antisense: GUUUGAUGACCGAAGGUCGUU (corresponds to base pairs 677–695 of *Aae comm2*). Previously described control siRNA (Nguyen et al., 2013) was used in these experiments; BLAST searches have confirmed that this siRNA does not have any known targets in the *A. aegypti* genome. For nerve cord phenotype assessments, at least eight replicate experiments were performed with each siRNA. Knockdown of *Aae comm2* was confirmed through *in situ* hybridization experiments in two separate replicate experiments. Knockdown of *Aae fra* was performed as previously described in two separate replicate experiments (Clemons et al., 2011).

Microarray experiments

Two complementary microarray experiments were used to assess the impacts of Fra signaling on global gene expression. In the first experiment, global gene expression profiles for stage 13 *fra[3]/fra[3]* mutant *Drosophila* vs. wild-type embryos were compared. Four replicates, each with 10 embryos for each condition (*fra[3]* mutant or wild-type) were prepared. The second experiment examined effects of activated NetA-Fra overexpression in the third instar wing imaginal disc. GFP-marked NetA+Fra overexpression wing discs were prepared as previously described (Flannery et al., 2010), and age matched wild type discs with GFP clones were used as controls. Four replicates with 15 discs for each condition (NetA+Fra or wild-type) were prepared. For each of the two microarray experiments, total RNA was isolated using Trizol LS Reagent (Invitrogen, Carlsbad, CA) according to the manufacturer's instructions. Total RNA was quantified by OD_{260}, and RNA quality was assessed using an Agilent 2100 Bioanalyzer.

RNA samples were sent to the University of Notre Dame Genomics and Bioinformatics Core Facility which performed hybridization experiments using the Affymetrix GeneChip *Drosophila* Genome 2.0 arrays (Affymetrix, Inc., Santa Clara, CA). RNA samples were processed and hybridized using the GeneChip 3′IVT Express kit (Affymetrix, Inc., Santa Clara, CA) according to the manufacturer's instructions. Briefly, reverse transcriptase and an oligo(dT) primer were used to synthesize first-strand cDNA. Second-strand cDNA was synthesized using DNA polymerase. Biotin-modified amplified RNA (aRNA) was generated through *in vitro* transcription. The aRNA was purified, fragmented, and then hybridized in a GeneChip Hybridization Oven 640 at 45° C for 16 hours. Finally, the microarrays were washed and stained in a GeneChip Fluidics Station 450 and scanned in a GeneChip 3000 7G scanner. Microarray data pre-processing and normalization were performed using the Bioconductor packages in R. Microarray data were deposited in the National Center for Biotechnology Information Gene Expression Omnibus under accession numbers GSE47112 (http://www.ncbi.nlm.nih.gov/geo/query/acc.cgi?acc=GSE47112, *fra* loss of function study) and GSE47113 (http://www.ncbi.nlm.nih.gov/geo/query/acc.cgi?acc=GSE47113; Net-Fra activation study).

Acknowledgments

Grant sponsors: NIH/NIAID Award R01-AI081795

University of Notre Dame Genomics and Bioinformatics Pilot Project Award

We are grateful to Ping Le who assisted with riboprobe preparation, as well as Charles Tessier and Lucy Shi who assisted with the *Drosophila* genetic crosses. We are grateful to Brent Harker for his assistance with the microarray experiments. Thanks to members of the lab for their advice and comments on the manuscript. M.D.S. and D.W.S. were funded by the National Institutes of Health. M.D.S., J.T., and E.Z. were funded by a University of Notre Dame Genomics and Bioinformatics Pilot Project Award.

References

Arensburger P, Megy K, Waterhouse RM, Abrudan J, Amedeo P, Antelo B, Bartholomay L, Bidwell S, Caler E, Camara F, Campbell CL, Campbell KS, Casola C, Castro MT, Chandramouliswaran I, Chapman SB, Christley S, Costas J, Eisenstadt E, Feschotte C, Fraser-Liggett C, Guigo R, Haas B, Hammond M, Hansson BS, Hemingway J, Hill SR, Howarth C, Ignell R, Kennedy RC, Kodira CD, Lobo NF, Mao C, Mayhew G, Michel K, Mori A, Liu N, Naveira H, Nene V, Nguyen N, Pearson MD, Pritham EJ, Puiu D, Qi Y, Ranson H, Ribeiro JM, Roberston HM, Severson DW, Shumway M, Stanke M, Strausberg RL, Sun C, Sutton G, Tu ZJ, Tubio JM, Unger MF, Vanlandingham DL, Vilella AJ, White O, White JR, Wondji CS, Wortman J, Zdobnov EM, Birren B, Christensen BM, Collins FH, Cornel A, Dimopoulos G, Hannick LI, Higgs S, Lanzaro GC, Lawson D, Lee NH, Muskavitch MA, Raikhel AS, Atkinson PW. Sequencing of *Culex quinquefasciatus* establishes a platform for mosquito comparative genomics. Science. 2010; 330:86–88. [PubMed: 20929810]

Behura SK, Haugen M, Flannery E, Sarro J, Tessier CR, Severson DW, Duman-Scheel M. Comparative genomic analysis of *Drosophila melanogaster* and vector mosquito developmental genes. PLoS One. 2011; 6:e21504. [PubMed: 21754989]

Bellen, et al. The *Drosophila* gene disruption project: progress using transposons with distinctive site specificities. Genetics. 2011; 188(3):731–743. [PubMed: 21515576]

Chenna R, Sugawara H, Koike T, Lopez R, Gibson TJ, Higgins DG, Thompson JD. Multiple sequence alignment with the Clustal series of programs. Nucleic Acids Res. 2003; 31:3497–3500. [PubMed: 12824352]

Choi, Y-J. Dissertation. The Ohio State University; 2003. Function of *commissureless* and related genes in *Drosophila* neural development.

Clemons A, Haugen M, Severson D, Duman-Scheel M. Functional analysis of genes in *Aedes aegypti* embryos. Cold Spring Harb Protoc. 2010a; 2010:2010. pdb prot5511.

Clemons, A.; Mori, A.; Haugen, M.; Severson, DW.; Duman-Scheel, M. Cold Spring Harb Protoc. 2010b. Culturing and egg collection of *Aedes aegypti*. 2010:pdb prot5507

Clemons A, Haugen M, Flannery E, Kast K, Jacowski C, Severson D, Duman-Scheel M. Fixation and preparation of developing tissues from *Aedes aegypti*. Cold Spring Harb Protoc. 2010c; 2010:2010. pdb prot5508.

Clemons A, Flannery E, Kast K, Severson D, Duman-Scheel M. Immunohistochemical analysis of protein expression during *Aedes aegypti* development. Cold Spring Harb Protoc. 2010d 2010:pdb prot5510.

Clemons A, Haugen M, Le C, Mori A, Tomchaney M, Severson DW, Duman-Scheel M. siRNA-mediated gene targeting in *Aedes aegypti* embryos reveals that frazzled regulates vector mosquito CNS development. PLoS One. 2011; 6:e16730. [PubMed: 21304954]

Cook RK, Christensen SJ, Deal JA, Coburn RA, Deal ME, Gresens JM, Kaufman TC, Cook KR. The generation of chromosomal deletions to provide extensive coverage and subdivision of the *Drosophila melanogaster* genome. Genome Biol. 2012; 13(3):R21. [PubMed: 22445104]

Davis C. A comparative study of larval embryogenesis in the mosquito *Culex fatigans wiedemann* (diptera: culicidae) and the sheep-fly *Lucilia sericata meigen* (diptera: calliphoridae). Australian Journal of Zoology. 1967; 15:547–579.

Dickson BJ. Molecular mechanisms of axon guidance. Science. 2002; 298:1959–1964. [PubMed: 12471249]

Dickson BJ, Gilestro GF. Regulation of commissural axon pathfinding by slit and its Robo receptors. Annu Rev Cell Dev Biol. 2006; 22:651–675. [PubMed: 17029581]

Duman-Scheel M, Patel NH. Analysis of molecular marker expression reveals neuronal homology in distantly related arthropods. Development. 1999; 126:2327–2334. [PubMed: 10225992]

Evans TA, Bashaw GJ. Slit/Robo-mediated axon guidance in *Tribolium* and *Drosophila*: divergent genetic programs build insect nervous systems. Dev Biol. 2012; 363:266–278. [PubMed: 22245052]

Felsenstein J. Estimating effective population size from samples of sequences: a bootstrap Monte Carlo integration method. Genet Res. 1992; 60:209–220. [PubMed: 1286805]

Flannery E, Vanzomeren-Dohm A, Beach P, Holland WS, Duman-Scheel M. Induction of cellular growth by the axon guidance regulators netrin A and semaphorin-1a. Dev Neurobiol. 2010; 70:473–484. [PubMed: 20162636]

Haugen M, Flannery E, Tomchaney M, Mori A, Behura SK, Severson DW, Duman-Scheel M. Semaphorin-1a is required for *Aedes aegypti* embryonic nerve cord development. PLoS One. 2011; 6:e21694. [PubMed: 21738767]

Haugen M, Tomchaney M, Kast K, Flannery E, Clemons A, Jacowski C, Simanton Holland W, Le C, Severson D, Duman-Scheel M. Whole-mount *in situ* hybridization for analysis of gene expression during *Aedes aegypti* development. Cold Spring Harbor Protocols. 2010 pdb prot5509.

Keleman K, Rajagopalan S, Cleppien D, Teis D, Paiha K, Huber LA, Technau GM, Dickson BJ. Comm sorts robo to control axon guidance at the *Drosophila* midline. Cell. 2002; 110:415–427. [PubMed: 12202032]

Keleman K, Ribeiro C, Dickson BJ. Comm function in commissural axon guidance: cell-autonomous sorting of Robo in vivo. Nat Neurosci. 2005; 8:156–163. [PubMed: 15657595]

Kidd T, Bland KS, Goodman CS. Slit is the midline repellent for the robo receptor in *Drosophila*. Cell. 1999; 96:785–794. [PubMed: 10102267]

Kolodziej PA, Timpe LC, Mitchell KJ, Fried SR, Goodman CS, Jan LY, Jan YN. frazzled encodes a *Drosophila* member of the DCC immunoglobulin subfamily and is required for CNS and motor axon guidance. Cell. 1996; 87:197–204. [PubMed: 8861904]

Kriventseva EV, Rahman N, Espinosa O, Zdobnov EM. OrthoDB: the hierarchical catalog of eukaryotic orthologs. Nucleic Acids Res. 2008; 36:D271–275. [PubMed: 17947323]

Lawson D, Arensburger P, Atkinson P, Besansky NJ, Bruggner RV, Butler R, Campbell KS, Christophides GK, Christley S, Dialynas E, Hammond M, Hill CA, Konopinski N, Lobo NF, MacCallum RM, Madey G, Megy K, Meyer J, Redmond S, Severson DW, Stinson EO, Topalis P, Birney E, Gelbart WM, Kafatos FC, Louis C, Collins FH. VectorBase: a data resource for invertebrate vector genomics. Nucleic Acids Res. 2009; 37:D583–587. [PubMed: 19028744]

McGovern VL, Seeger MA. Mosaic analysis reveals a cell-autonomous, neuronal requirement for Commissureless in the *Drosophila* CNS. Dev Genes Evol. 2003; 213:500–504. [PubMed: 12928898]

Metaxakis A, Oehler S, Kliakis A, Savakis C. Minos as a genetic and genomic tool in *Drosophila melanogaster*. Genetics. 2005; 171(2):571–581. [PubMed: 15972463]

Nene V, Wortman JR, Lawson D, Haas B, Kodira C, et al. Genome sequence of *Aedes aegypti*, a major arbovirus vector. Science. 2007; 316:1718–1723. [PubMed: 17510324]

Nguyen C, Andrews E, Le C, Sun L, Annan Z, Clemons A, Severson DW, Duman-Scheel M. Functional genetic characterization of salivary gland development in *Aedes aegypti*. Evodevo. 2013; 4:9. [PubMed: 23497573]

Patel, N. *In situ* hybridization to whole mount *Drosophila* embryos. New York: Wiley-Liss; 1996. p. 357-370.

Patel NH. Imaging neuronal subsets and other cell types in whole-mount *Drosophila* embryos and larvae using antibody probes. Methods Cell Biol. 1994; 44:445–487. [PubMed: 7707967]

Philipp M, Niederkofler V, Debrunner M, Alther T, Kunz B, Stoeckli ET. RabGDI controls axonal midline crossing by regulating Robo1 surface expression. Neural Dev. 2012; 7:36. [PubMed: 23140504]

Ricard CS, Jakubowski JM, Verbsky JW, Barbieri MA, Lewis WM, Fernandez GE, Vogel M, Tsou C, Prasad V, Stahl PD, Waksman G, Cheney CM. *Drosophila* rab GDI mutants disrupt development but have normal Rab membrane extraction. Genesis. 2001; 31:17–29. [PubMed: 11668674]

Saitou N, Nei M. The neighbor-joining method: a new method for reconstructing phylogenetic trees. Mol Biol Evol. 1987; 4:406–425. [PubMed: 3447015]

Seeger M, Tear G, Ferres-Marco D, Goodman CS. Mutations affecting growth cone guidance in *Drosophila*: genes necessary for guidance toward or away from the midline. Neuron. 1993; 10:409–426. [PubMed: 8461134]

Smedley D, Haider S, Ballester B, Holland R, London D, Thorisson G, Kasprzyk A. BioMart--biological queries made easy. BMC Genomics. 2009; 10:22. [PubMed: 19144180]

Stein E, Tessier-Lavigne M. Hierarchical organization of guidance receptors: silencing of netrin attraction by slit through a Robo/DCC receptor complex. Science. 2001; 291:1928–1938. [PubMed: 11239147]

Tamura K, Dudley J, Nei M, Kumar S. MEGA4: Molecular Evolutionary Genetics Analysis (MEGA) software version 4.0. Mol Biol Evol. 2007; 24:1596–1599. [PubMed: 17488738]

Tear G, Harris R, Sutaria S, Kilomanski K, Goodman CS, Seeger MA. commissureless controls growth cone guidance across the CNS midline in *Drosophila* and encodes a novel membrane protein. Neuron. 1996; 16:501–514. [PubMed: 8785048]

Tweedie S, Ashburner M, Falls K, Leyland P, McQuilton P, Marygold S, Millburn G, Osumi-Sutherland D, Schroeder A, Seal R, Zhang H. FlyBase: enhancing *Drosophila* Gene Ontology annotations. Nucleic Acids Res. 2009; 37:D555–559. [PubMed: 18948289]

VanZomeren-Dohm A, Flannery E, Duman-Scheel M. Whole-mount in situ hybridization detection of mRNA in GFP-marked *Drosophila* imaginal disc mosaic clones. Fly (Austin). 2008; 2:323–325. [PubMed: 19029797]

Wolf B, Seeger MA, Chiba A. Commissureless endocytosis is correlated with initiation of neuromuscular synaptogenesis. Development. 1998; 125:3853–3863. [PubMed: 9729493]

Yang L, Garbe DS, Bashaw GJ. A frazzled/DCC-dependent transcriptional switch regulates midline axon guidance. Science. 2009; 324:944–947. [PubMed: 19325078]

Zuckerkandl, E.; Pauling, L. Evolutionary divergence and convergence in the proteins. In: Vogel, VBaHJ., editor. Evolving Genes and Proteins. New York: Academic Press; 1965. p. 97-166.

Key Findings

- The vector mosquitoes *Aedes aegypti* and *Culex quinquefasciatus* possess *commissureless2 (comm2)* genes (one and three, respectively) that are expressed by commissural axons during embryonic nerve cord development.
- Knockdown of *A. aegypti commissureless2 (Aae comm2)*, the single *comm* family ortholog in *A. aegypti*, results in a commissureless phenotype that phenocopies the *frazzled (fra)* loss of function phenotype in this species.
- Mutation of *D. melanogaster comm2*, an ortholog of *Aae comm2*, also results in a commissureless phenotype which bears resemblance to the *fra* loss of function mutant.
- Loss of Frazzled signaling in *A. aegypti* or *D. melanogaster* results in decreased *comm2* expression, suggesting that Comm2 functions to mediate the conserved ability of Fra to downregulate repulsion in precrossing commissural axons of both species.

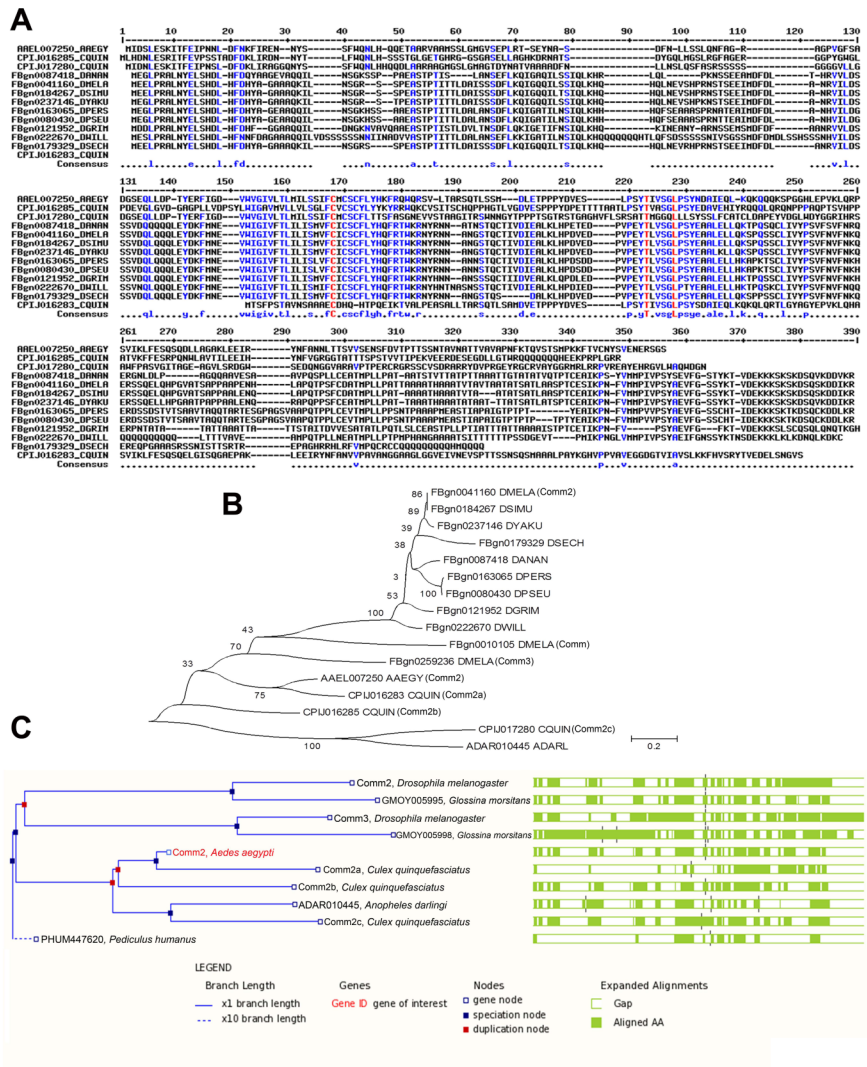

Fig. 1. Sequence analysis of insect Comm family proteins

A. A partial multiple alignment of deduced amino acid sequences of the N-termini of predicted *comm2* orthologs among mosquito and fruit fly species is shown. The gene accession numbers and species are indicated to the left of the sequences in the alignment. The amino acid position of aligned sequences is indicated at the top, while the consensus sequence of the alignment is shown below the aligned sequences. B. A neighbor-joining phylogenetic tree of *C. quinquefasciatus* Comm proteins along with orthologous proteins identified in *A. aegypti* and *Drosophila* species is shown. All three Comm family proteins of *D. melanogaster* (Comm, Comm2, and Comm3) are included in the tree. The percentage of replicate trees in which proteins clustered together through bootstrap testing is shown next to the branches. The tree is drawn to scale, with branch lengths in the same units as those of the evolutionary distances used to infer the phylogenetic tree. The scale of the evolutionary distances as units of the number of amino acid substitutions per site is shown. C. The amino acid sequence conservation of selected orthologs of AAEL007250, as inferred from the GBrowse tool of VectorBase (2009), shown at right corresponds to the phylogenetic relationships among the proteins shown on the left. The percentages of sequence identities, sequence gaps and details of tree nodes are shown below the figure as captions generated by Gbrowse. Abbreviations in this figure are as follows: *A. aegypti* = AAEGY, *C.*

quinquefasciatus = CQUIN, *D. ananassae* = DANAN, *D. melanogaster* = DMELA, *D. simulans* = DSIMU, *D. yakuba* = DYAKU, *D. persimilis* = DPERS, *D. pseudoobscura* = DPSEU, *D. grimshawi* = DGRIM, *D. willistoni* = DWILL, *D. sechellia* = DSECH.

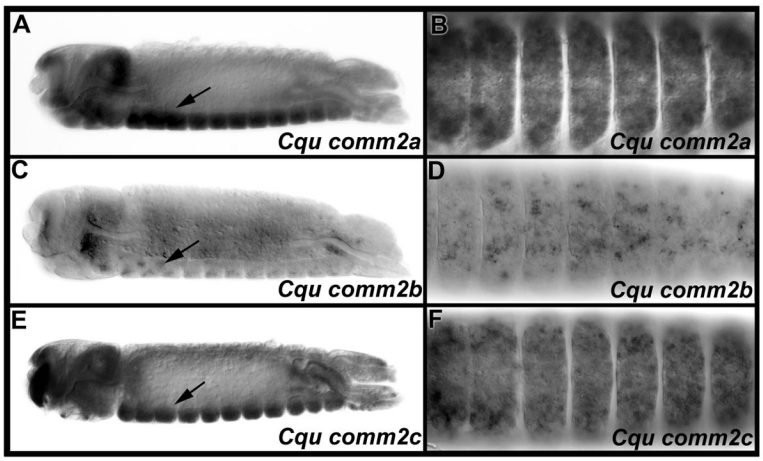

Fig. 2. Three *C. quinquefasciatus comm* family genes are expressed in the developing nerve cord

Cqu comm2a (A, B), *Cqu comm2b* (C, D), and *Cqucomm2c* (E, F) transcripts are detected in the developing *C. quinquefasciatus* nerve cord and head region (both brain and overlying tissue). Arrows mark nerve cord expression on the ventral sides of 22 hour old embryos; lateral views oriented anterior left and ventral down are shown. Ventral views of CNS expression in these same animals (B, D, F; anterior is again oriented left) are shown to the right of panels A, C, and E, respectively. All three genes are widely expressed in the developing nerve cord during the period of commissural axon guidance, but the neural expression levels of *Cqu comm2b* (F) are markedly less than the neural expression levels of the other two *comm*2 genes (B, D).

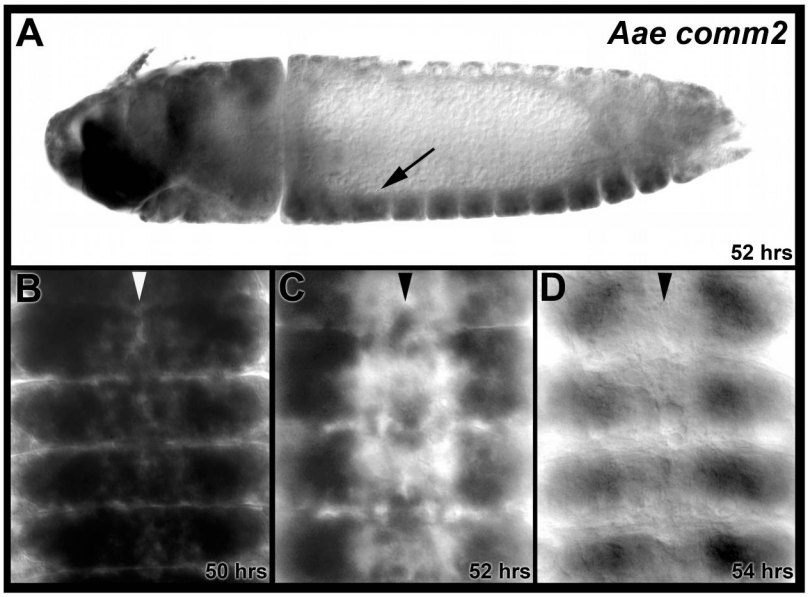

Fig. 3. *Aae comm2* is expressed in the developing nerve cord

Aae comm2 expression is detected during *A. aegypti* embryonic ventral nerve cord development. (A) An arrow marks nerve cord expression in a lateral view of a 52 hour old embryo oriented anterior left and ventral down. Transcripts are also detected in the brain and overlying head tissue. (B–D) Transcript levels peak in the ventral nerve cord at 50 hours (B) and are observed in a more restricted set of neurons by 52 hours (C). At 54 hours (D), when most commissural axons have crossed the midline, expression in the nerve cord has diminished. Filleted nerve cords oriented anterior upward are shown in B–D, in which the midline is marked by arrowheads.

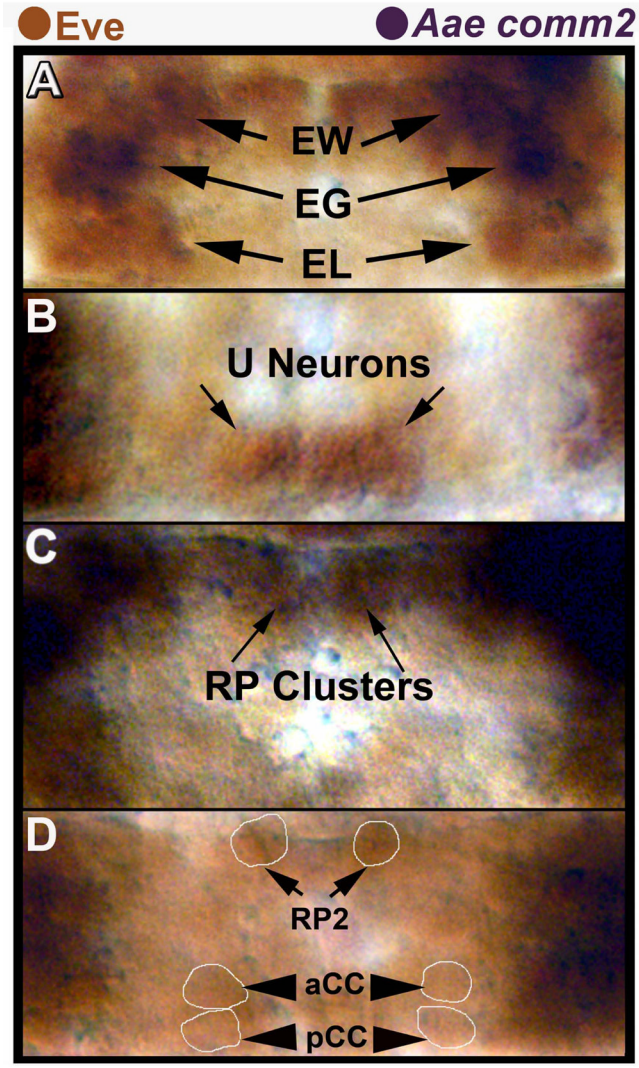

Fig. 4. Lack of *Aae comm2* expression in neurons that do not cross the midline

The EL (A) and U (B) neuron clusters, RP2, aCC, and pCC neurons (D) are marked by expression of Eve protein (brown). These Eve-positive neurons do not express *Aae comm2* mRNA (dark purple, A–D), and their axons do not cross the midline. The EG, EW (A) and RP neuron (RP1, 3, 4; RP2 is out of focus) clusters (C) were positionally identified with respect to Eve-positive neurons; these neurons (with the exception of RP2) project axons to the midline and express *Aae comm2* (dark purple). All images are oriented anterior upward and correspond to different segments/focal planes of the nerve cord from a single filleted 51 hour old embryo. Ventral focal planes of the nerve cord are shown in A and B, while C shows a more dorsal plane of focus. Panel D shows the dorsal-most plane of focus in this nerve cord. Light Eve staining permitted examination of *comm2* expression in Eve-positive neurons of *A. aegypti* embryos in which tissue autofluorescence hinders fluorescent immunohistochemistry. Lightly-stained Eve-positive cell bodies were circled in some panels (D) to facilitate interpretation of these data.

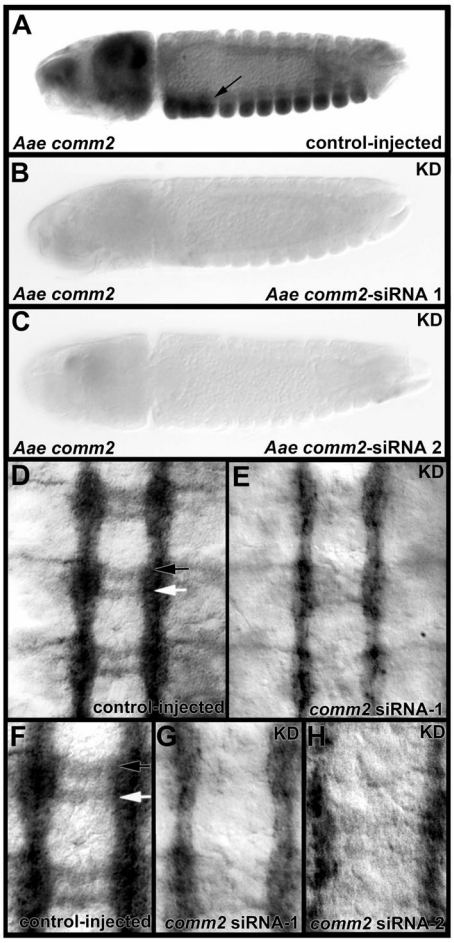

Fig. 5. Knockdown of *Aae comm2* results in a commissureless phenotype

Aae comm2 knockdown (KD) was confirmed through whole-mount *in situ* hybridization, which demonstrated that two siRNAs targeting *comm2*, siRNA-1 (B) and siRNA-2 (C), resulted in loss of *comm2* transcripts throughout the entire embryo, including the nerve cord. *comm2* levels were not noticeably altered by injection of control siRNA (A, arrow marks ventral nerve cord expression). Lateral views are shown in panels A–C which are oriented anterior left and ventral downward. In D–H, anti-acetylated tubulin staining marks the axons in the filleted ventral nerve cords (oriented anterior upward) of control siRNA-injected (D, F) and *comm2* knockdown siRNA-injected (E, G, H) embryos at 53 hours of development. In control-injected nerve cords (D, F), which have a wild-type appearance, the anterior commissure is marked by a black arrow while a white arrow marks the posterior commissure. Knockdown of *comm2* results in loss of commissural axons (E, G, H). Comparable results were obtained with two different siRNAs (*comm2* siRNA-1 in E, G; *comm2* siRNA-2 in H). Panels F and G show high magnification views of the nerve cords in D and E, respectively.

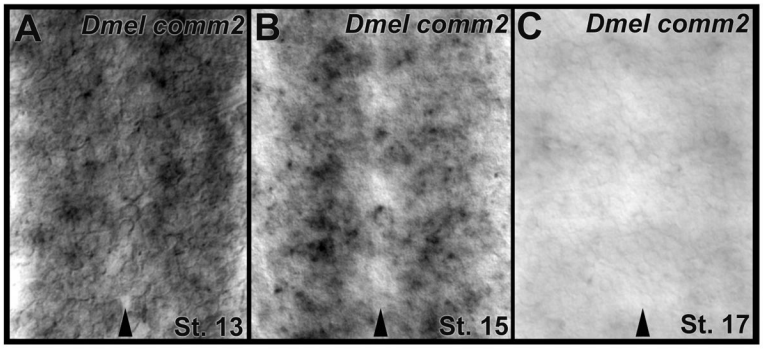

Fig. 6.

Expression of *comm2* during *D. melanogaster* nerve cord development. *comm2* expression is detected during *D. melanogaster* embryonic ventral nerve cord development. High levels of transcript are detected at Stage 13 (A) and are observed in a more restricted set of neurons at Stage 15 (B). By stage 17 (C), when most commissural axons have crossed the midline, expression in the nerve cord has significantly diminished. Arrowheads in A–C mark the midline; filleted nerve cords are oriented anterior upward in these panels.

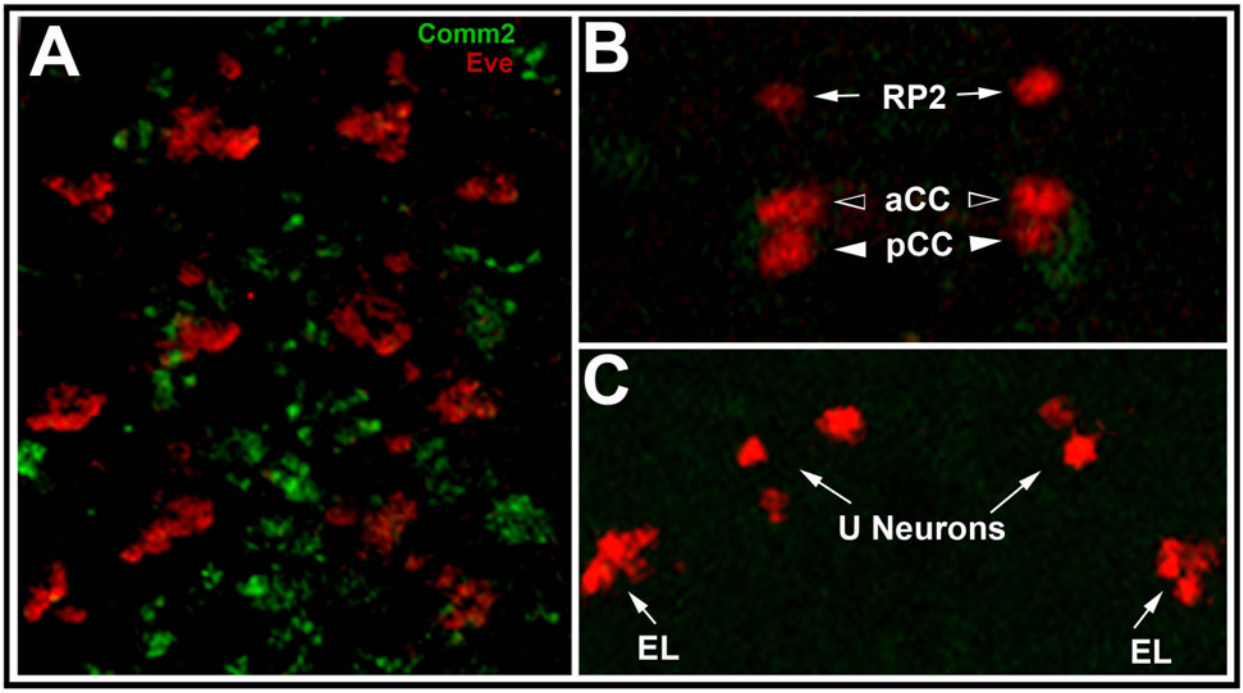

Fig. 7.

Lack of *D. melanogaster* Comm2 expression in axons that do not cross the midline. (A) Non-overlapping expression of Eve (red) and Comm2 (green, *MB01146* reporter) in a stage 14 *D. melanogaster* embryo. Three abdominal segments of a maximum projection image of the nerve cord which is oriented anterior upward are shown. No Comm2 expression is detected in the Eve-positive RP2, aCC, pCC (B), U and EL neurons (C), none of which project axons to the midline. Anterior is oriented upward in all panels. A single section through a dorsal focal plane of the posterior-most segment of A is shown in B, while a single section through a ventral portion of this same segment is shown in C.

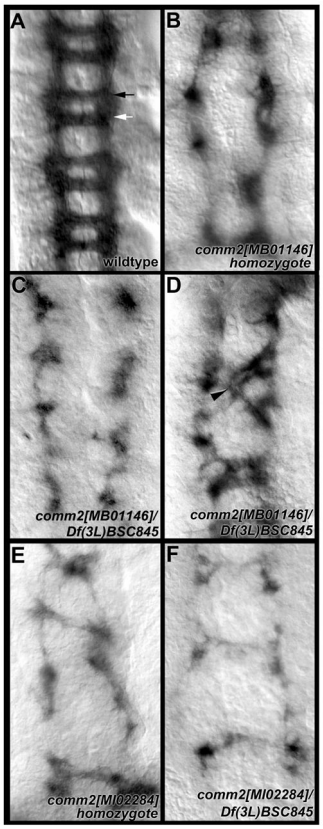

Fig. 8. Loss of *D. melanogaster comm2* function results in a commissureless phenotype

P102 staining marks axons of the ventral nerve cord in wild-type (A) and *comm2* mutant (B–F) embryos. Significant commissure loss, as well as longitudinal breaks, are observed in *comm2* mutants (B–F), in which the overall appearance of the nerve cord is generally distorted. Genotypes are noted in each panel. Commissure loss phenotypes are quantified for each genotype in Table 3. The black arrow in A marks the anterior commissure, while the white arrow marks the posterior commissure. In D, the arrowhead marks axons that have extended across the segmental boundary. Stage 15 nerve cords oriented anterior upward are shown in each panel.

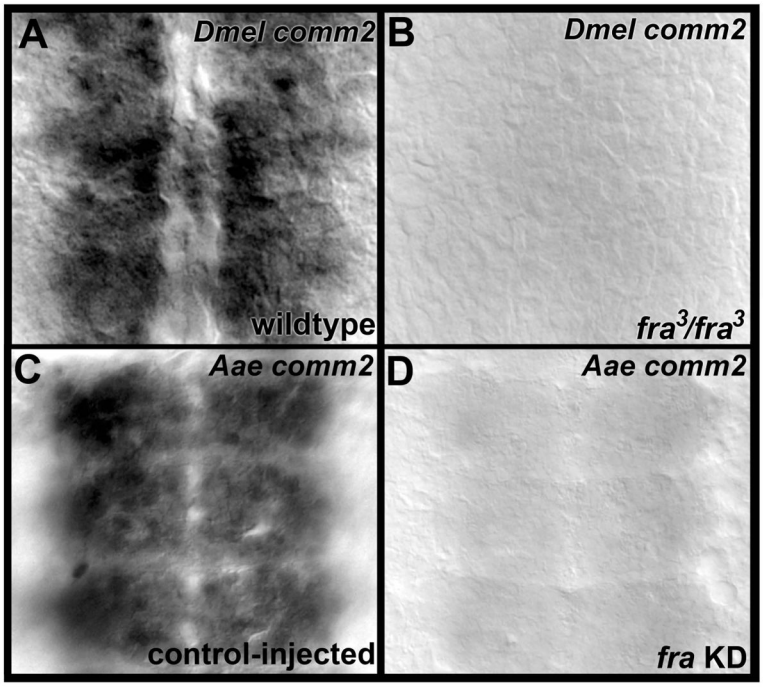

Fig. 9. Loss of *fra* function results in decreased *comm2* transcripts

Loss of *fra* function results in decreased *comm2* transcript levels in both *D. melanogaster* (B) and *A. aegypti* (D). A wild-type *D. melanogaster* embryo (A) and control-injected *A. aegypti* embryo (B) are included for comparison. Filleted nerve cords of stage 13 *D. melanogaster* embryos (A, B) and 49 hour old *A. aegypti* embryos (C, D) in which the anterior ends are oriented upward are shown.

Table 1

Pairwise distances between genes calculated using MEGA4. The number of amino acid substitutions per site from analysis between sequences is shown. 1: AAEL007250_AAEGY, 2: CPIJ016285_CQUIN, 3: CPIJ017280_CQUIN, 4: FBgn0087418_DANAN, 5: FBgn0121952_DGRIM, 6: FBgn0041160_DMELA, 7: FBgn0163065_DPERS, 8: FBgn0080430_DPSEU, 9: FBgn0179329_DSECH, 10: FBgn0184267_DSIMU, 11: FBgn0222670_DWILL, 12: FBgn0237146_DYAKU, 13: CPIJ016283_CQUIN. These species abbreviations are defined in the legend of Fig. 1.

	1	**2**	**3**	**4**	**5**	**6**	**7**	**8**	**9**	**10**	**11**	**12**	**13**
1													
2	1.1												
3	1.3	2.0											
4	1.3	1.9	2.2										
5	1.3	1.8	2.4	0.3									
6	1.3	1.7	2.2	0.2	0.3								
7	1.4	2.0	2.4	0.2	0.3	0.2							
8	1.4	2.0	2.4	0.2	0.3	0.2	0.0						
9	1.5	1.6	2.2	0.4	0.5	0.3	0.4	0.4					
10	1.3	1.8	2.2	0.2	0.3	0.0	0.2	0.2	0.2				
11	1.3	1.8	2.4	0.3	0.3	0.3	0.3	0.3	0.6	0.3			
12	1.3	1.8	2.2	0.2	0.3	0.0	0.2	0.2	0.3	0.0	0.3		
13	0.5	1.4	1.6	1.5	1.5	1.5	1.7	1.7	1.6	1.4	1.6	1.5	

Table 2

A. aegypti comm2 knockdown phenotypes. 53 hour old embryos were assessed post-injection of *comm2*-siRNA 1, *comm2*-siRNA 2, or control siRNA. Commissure loss phenotypes were scored in individual segments following anti-acetylated tubulin staining. Percentages of segments with wildtype, moderate (thinning of commissures), or severe (loss/near loss of commissures) phenotypes are indicated. Data were compiled from three or more replicate experiments.

	n	% segments with no commissure defects	% segments with moderate commissure defects	% segments with severe commissure defects
control-injected	58	98	2	0
***comm2*-siRNA 1**	42	5	21	74
***comm2*-siRNA 2**	81	2	21	77

Table 3

D. melanogaster comm2

knockdown commissure loss phenotypes. BP102-stained stage 15–16 *D. melanogaster* embryos were assessed for commissure loss phenotypes. Percentages of segments with wildtype, moderate (thinning of commissures) or severe (loss/near loss of commissures) phenotypes are indicated. Data were compiled from three or more replicate experiments.

	n	% segments with no commissure defects	% segments with moderate commissure defects	% segments with severe commissure defects
wildtype	110	100%	0%	0%
comm2[MB01146]/comm2[MB01146]	65	0%	6%	94%
comm2[MB01146]/Df(3L)BSC845	47	0%	11%	89%
comm2[MI02284]/comm2[MI02284]	107	3%	26%	71%
comm2[MI02284]/Df(3L)BSC845	54	0%	22%	78%